TRANSACTIONS OF THE INSTITUTE OF FLUID-FLOW MACHINERY

No. 121, 2008, 33-48

KAZIMIERZ RUP*, MAREK GARGULA and PIOTR SARNA

Numerical simulation of turbulent flow through a square-sectioned duct with a 90-degree bend using FLUENT

Cracow University of Technology, Institute of Process and Power Engineering, Al. Jana Pawła II 37, 31-864 Kraków

Abstract

The turbulent flow in a square-sectioned duct with an installed bend was investigated numerically. The calculations were based on two different turbulence models, namely the standard k-ε model and the k-ω SST model. The numerical computations were carried out using the commercial software package FLUENT 6.1. Numerical results for velocity, turbulent intensity and pressure distributions are presented. The obtained results of numerical calculations are compared with corresponding results of experimental studies available in references. The comparative analysis of the obtained numerical results and experimental ones, proved a high degree of their consistency.

Keywords: Turbulent flow; Air; Water; Square-sectioned duct; Bend

Nomenclature

a	–	dimension of duct wall, m
c_p	–	pressure coefficient
De	–	Dean number
$D_h = a$	–	hydraulic diameter, m
k	–	turbulence kinetic energy, m^2/s^2
L_{inlet}	–	longitudinal distance along duct axis before the elbow, m

*Corresponding author. E-mail address: krup@riad.usk.pk.edu.pl

L_{outlet}	–	longitudinal distance along duct axis after the elbow, m
$\bar{p}$	–	mean static pressure, Pa
p_o	–	pressure at the outer side of the elbow duct, Pa
p_i	–	pressure at the inner side of the elbow duct, Pa
p_{ref}	–	reference value of $\bar{p}$, i. e., $\bar{p}$ at $x' = 0$; $y' = a/2$; $z' = 0$, Pa
R	–	elbow curvature radius, m
Re	–	Reynolds number based on spatial mean velocity and hydraulic diameter
Tu	–	turbulence intensity, %
U	–	time-averaged velocity in x direction, m/s
v_i'	–	instantaneous (fluctuating) velocity in i direction, m/s
$\bar{v}_i$	–	time-averaged velocity in i direction, m/s
v_τ	–	friction velocity, m/s
V	–	time-averaged velocity in y direction, m/s
V_c	–	longitudinal velocity component averaged in cross section, m/s
x, y, z	–	coordinates, m
y^+	–	non dimensional length from wall surface

Greek symbols

μ	–	dynamic viscosity of fluid, kg/ms
ρ	–	density of fluid, kg/m^3
Φ	–	elbow angle, deg
ω	–	specific rate of kinetic energy dissipation, 1/s

1 Introduction

Square-sectioned ducts with installed bends frequently occur in many installations of heat power engineering. Examples of such systems are supply installations of gaseous mediums to burners, gas turbines, exhaust installations, etc.

Pressure fields in flows through pipes and rectangular ducts show considerable level of homogeneity in particular cross sections. On the other hand in flows through similar ducts with installed bends, velocity as well as pressure fields show high level of complexity. Momentum forces that act on the bend cause large pressure gradients in the direction from inner to outer wall. Areas of vorticity forming directly in front of and after the bend are responsible for the so called secondary flows in the domain of the bend and result in additional pressure losses.

Considering the frequent occurrence of described flows in nature, they were subject of many theoretical as well as experimental studies that can be found in references [1÷3]. Majority of those studies focus on a simpified cases based on the assumption of a fully developed flow field at the inlet or large radiuses of the bend. One of the most important studies concerning development of hydrodynamic flows in a square-sectioned duct with the installed bend having a mean radius $R/D_h = 2.3$ is described in Ref. [2]. In this study, measurements of local longitudinal and cross components of water velocity were carried out using LDV technique for laminar (Re = 790) and turbulent (Re = 40000) flows. Measurements of static pressure were made in selected areas of the bend.

Turbulent flow of air through a square-sectioned duct (80×80 mm) with an installed bend was the subject of study in Ref. [3]. Mean radius of the bend was $R/D_h = 2.0$ and the Reynolds number for the flow was Re = 40000 [3]. In order to measure the time averaged components of velocity field and its fluctuations values a hot wire technique was used [3]. In Ref. [4] the results of numerical simulations of flow through a duct with installed square-sectioned U-bend are presented. The mean radius of U-bend ($\phi = 180^{\circ}$) was $R/D_h = 0.65$. For numerical computations of the analyzed flow (Re = 100000) a 2-equation nonlinear (low-Re) $k-\omega$ turbulence model was used. For measurements of fluid flow in the area of the square-sectioned (150×150 mm) duct with two bends mounted in series, the flow visualization techniques were used [5]. Additionally, the measurements of static pressure were made on the mean lines of opposite vertical walls of the S-shaped duct [5].

In the present study time averaged fields of velocity components and pressure, as well as components of turbulence stress tensor in a developing hydrodynamic flow through a square-sectioned duct with an installed bend were numerically determined. For numerical simulations FLUENT [6], a commercially available software package was used. Obtained results were subject to detailed verification by comparing them with corresponding experimental results found in Ref. [2, 3]. Results obtained from these references were obtained for two different fluids (air and water) and different dimensions of flow ducts.

2 Mathematical model of analyzed turbulent flow

To intensify the processes of momentum, heat and mass transfer, most occurring flows show a turbulent nature. It is known that turbulent flows are characterized by fast changing random fluctuations of velocity, pressure, temperature and other quantities. To describe turbulent flows, a known procedure of averaging in time of these quantities was used [7, 8]. Assuming that the flows are non compressible and statistically stationary flow, the time averaged equations resulting from mass and momentum conservation equations have the following form:

$$\frac{\partial \overline{v_i}}{\partial x_i} = 0\,, \tag{1}$$

$$\rho \frac{\partial}{\partial x_j}\left(\overline{v}_i \overline{v}_j\right) = \frac{\partial}{\partial x_j}\left[-\bar{p}\delta_{ij} + \mu\left(\frac{\partial \overline{v}_i}{\partial x_j} + \frac{\partial \overline{v}_j}{\partial x_i}\right) - \rho\overline{v_i' v_j'}\right]. \tag{2}$$

The last term on the right side of equation (2) expresses the components of the Reynolds stress tensor:

$$R_{ij} = -\rho\overline{v_i' v_j'}\,. \tag{3}$$

Appearance of additional term in the equation of turbulent flow Eq. (3), causes that the system of Eqs. (1) and (2) becomes an open one. For unique description of the fluid motion additional relations determining the components of turbulent stress tensor (3) must be taken into consideration. To determine these components two different 2-equation turbulence models were used, namely the standard 2-equation $k-\varepsilon$ model and the $k-\omega$ SST model. These models belong to the group of viscous models available in FLUENT [6]. To obtain a unique description of the investigated flow, the following boundary conditions were formulated: zeroing of the velocity vector and turbulent kinetic energy on the walls, assumed value of the mean flow velocity, turbulence intensity Tu_o at the inlet to the duct and the length scale l. Turbulence intensity and length scale were defined by the following relations:

$$Tu_o = 0.16(\mathrm{Re})^{-1/8}\,, \tag{4}$$

$$l = 0.07D_h\,. \tag{5}$$

Values of the rate of dissipation of kinetic energy ε and the corresponding specific rate ω result from the assumed value of turbulence intensity Tu_o at the inlet cross section and the assumed changes of kinetic turbulent energy for the given model [6, 7].

To solve the system of differential equations resulting from mass and momentum equations and equations describing the model of turbulence, a method of finite volumes available in FLUENT was used. The flow space including the straight part of the rectangular inlet duct (L_{inlet}), the duct bend, and the straight outlet section of the duct (L_{outlet}), of the same cross dimensions were divided into a series of finite volumes as shown in Fig. 1b. The mesh was finer near the walls of the duct where large gradients of computed quantities were expected. The separated finite volumes were quadrilateral. Figure 1 shows a schematic of the flow test section along with a mesh in the inlet section of the duct.

Ratios of the smallest element adjacent to the duct wall to the hydraulic diameter for duct I ($a\times a = 80\times 80$ mm) and for duct II ($a\times a = 40\times 40$ mm) were $\delta_x^{(I)}/D_h = \delta_x^{(II)}/D_h = 0.00025$. In both cases the growth factor (ratio of preceding element to the next element) equaled 1.5. The lengths of straight sections of the duct depended on the cross section of the duct and were: $L_{inlet}^{(I)} = 1600$ mm, $L_{outlet}^{(I)} = 800$ mm and $L_{inlet}^{(II)} = 300$ mm, $L_{outlet}^{(II)} = 2000$ mm. To evaluate the quality of the generated finite volumes lattices, the skewness coefficient q is used in [6]. Value of coefficient $q = 0$, which is the most desirable case, corresponds to all angles of the cell being equal, whereas $q = 1$ corresponds to the entirely degenerated cell. Degenerated cells are characterized by coplanar orientation of the mesh nodes. These cells have a large influence on accuracy and stability of numerical calculations, thus it is recommended [6] that $q < 0.9$. Finite volumes

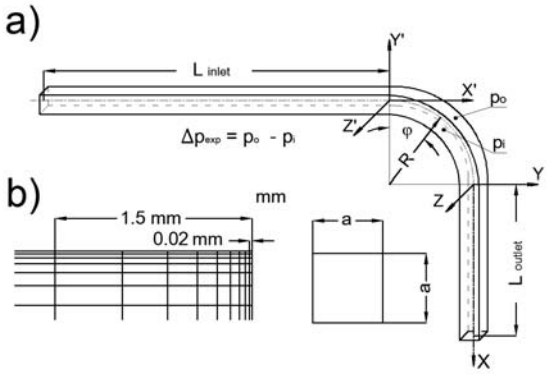

Figure 1. Geometry dimensions and mesh in the boundary layer of the volume.

generated in this study were characterized by a small value of skewness coefficient: $q < 0.5$. Thus, it can be accepted that the generated mesh of the integral volume is of good quality. It is also worth mentioning that the total number of finite volumes for the test duct I equaled 1766079, whereas the number of the mesh nodes totalled to 1838720. FLUENT [6] allows modeling of the boundary layer in case of turbulent flow via two methods. The first method, called the wall functions is based on algebraic relationships connecting the boundary region with the region of developed turbulent flow [6÷8]. Use of the second method allows obtaining more accurate results however, it requires a greater congestion of mesh elements near the wall. In this study, options available in FLUENT of full modeling of the boundary layer were used. During numerical calculations the dimensionless value of distance from the wall y^+ defined by equations [6÷8] was controlled.

$$y^+ = \frac{\rho v_\tau y}{\mu}\,. \tag{6}$$

Peak values of the y^+ parameter obtained through calculations occur in the sub area of the outlet cross section and the sub area of the outer wall bend. Those values were however much smaller than the ones suggested by FLUENT user manual to be $y^+ \leq 5$.

3 Discussion of the obtained numerical results

Numerical simulations were carried out using FLUENT [6] running on a two processor personal computer.

Two ducts of different lengths and different dimensions of cross sections were investigated. Duct I had the following dimensions: $(a \times a)^I = 80 \times 80$ mm, $L^{(I)}_{inlet} =$

1600 mm, $L_{outlet}^{(I)} = 800$ mm, $(R/D_h)^{(I)} = 2.0$. For this duct, the fluid thermophysical parameters of air were assumed as the appropriate experimental results were available. Duct II had the following dimensions: $(a \times a)^{II} = 40 \times 40$ mm, $L_{inlet}^{(II)} = 300$ mm, $L_{outlet}^{(II)} = 2000$ mm $(R/D_h)^{(II)} = 2.3$. In this case, for the same reason as above, water was chosen as examined fluid. In both cases the thermophysical properties of fluids were equivalent to those at standard temperature ($t = 20^{\circ}$C). The air Reynolds number referred to the hydraulic diameter of the duct had the following values: $\mathrm{Re}_1^{(I)} = 40000$, $\mathrm{Re}_2^{(I)} = 54054$, $\mathrm{Re}_3^{(I)} = 81081$. Reynolds number values for the flow of water were: $\mathrm{Re}_1^{(II)} = 40000$, $\mathrm{Re}_2^{(II)} = 60000$, $\mathrm{Re}_3^{(II)} = 80000$. In the analysis of flows through curved ducts the Dean number is used frequently. It is defined according to equation [1÷3]:

$$\mathrm{De} = \mathrm{Re}\sqrt{\frac{D_h}{2R}}. \tag{7}$$

Considering the Reynolds number values mentioned above, hydraulic diameter (D_h) and mean radii of bends the corresponding values of Dean number were: $\mathrm{De}_1^{(I)} = 20000$, $\mathrm{De}_2^{(I)} = 27027$, $\mathrm{De}_3^{(I)} = 40540$ and $\mathrm{De}_1^{(II)} = 18650$, $\mathrm{De}_2^{(II)} = 27975$, $\mathrm{De}_3^{(II)} = 37300$.

The obtained results are presented graphically in Figs. 2 to 9 for flow of air through duct I, and Figs. 10 to 15 for flow of water through duct II. Figure 2 represents dimensionless profiles of longitudinal velocity components of air in the cross section of the duct located one hydraulic diameter upstream from the duct bend: $x'/D_h = -1.0$. This cross section is also described by the coordinate: $z'/D_h = 0.0$. Continuous lines with squares and rhombs present results for simulations carried out using the $k-\varepsilon$ and $k-\omega$ SST turbulence models respectively.

The Reynolds number for the discussed flow was $\mathrm{Re}_1^{(I)} = 40000$ ($\mathrm{De}_1^{(I)} = 20000$). For comparison, corresponding experimental results found in Ref. [3] are presented as discrete points (black filled circles).

Profiles of the U/Vc velocity component for the same flow for cross section of the bend described by angular coordinate $\phi = 30^{\circ}$ ($z/D_h = 0.0$) are shown in Fig. 3. Very good compatibility of numerically obtained results (solid lines) with corresponding experimental results (black filled circles) found in Ref. [3] can be easily noticed.

Profiles of U/Vc velocity component of the discussed flow determined in the cross section of the bend for angular coordinate $\phi = 60^{\circ}$ ($z/D_h = 0.0$) are shown in Fig. 4. Similarly as in Fig. 3, the numerically obtained results correspond very well to the experimental values (black filled circles) found in Ref. [3].

In Figs. 3 and 4 the inner wall of the bend (smaller radius) is denoted with negative values of the y coordinate (on the y axis).

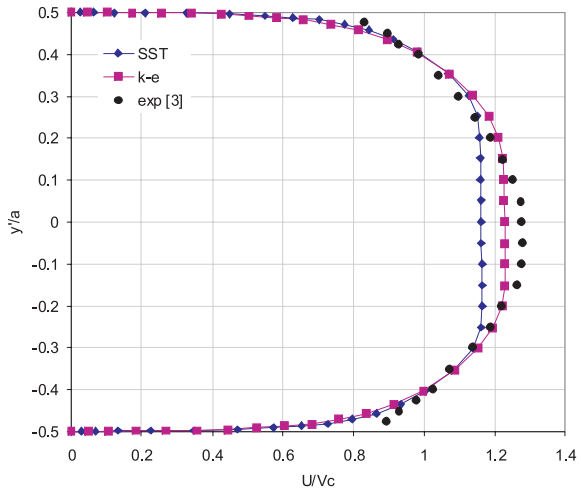

Figure 2. Comparison of velocity profiles obtained with $k-\omega$ SST and $k-\varepsilon$ models with experimental results for $x'/D_h = -1.0$; $z'/D_h = 0.0$.

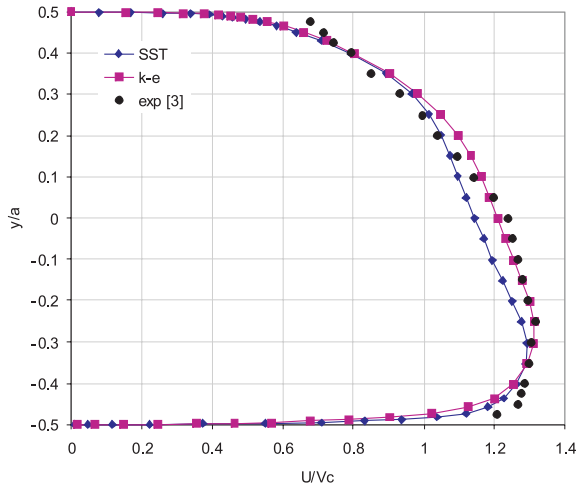

Figure 3. Comparison of velocity profiles obtained with $k-\omega$ SST and $k-\varepsilon$ models with experimental results for $\phi = 30^{\circ}$ ($z/D_h = 0.0$).

Clearly deformed profiles of U/Vc velocity component for the air flow ($\mathrm{Re}_1^{(I)} = 40000$) can be seen in Fig. 5. These profiles correspond to the cross section of the duct located one hydraulic diameter downstream of the duct bend ($x/D_h = 1.0$, $z/D_h = 0.0$). It seems that the qualitative changes of the U/Vc velocity

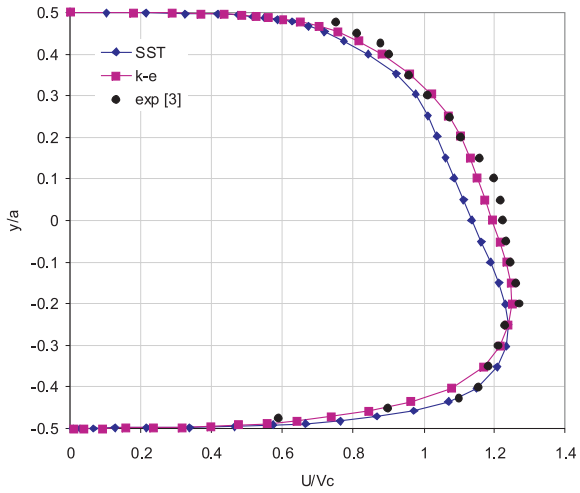

Figure 4. Comparison of velocity profiles obtained with $k-\omega$ SST and $k-\varepsilon$ models with experimental results for $\phi = 60^{\circ}$ $(z/D_h = 0, 0)$.

component in this case are better approximated by the $k-\omega$ SST turbulence model (rhombs) than the standard $k-\varepsilon$ turbulence model (squares).

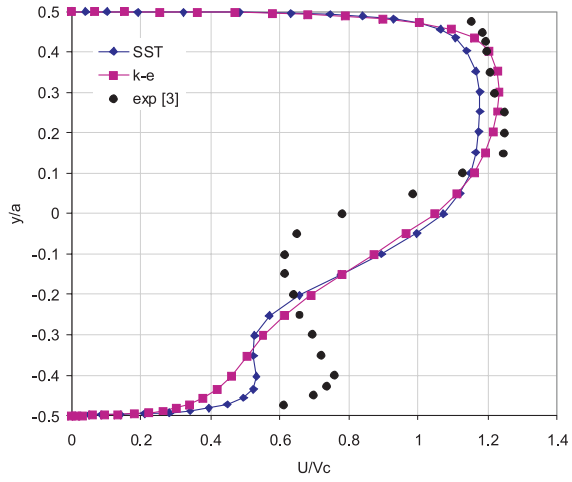

Figure 5. Comparison of velocity profiles obtained with $k-\omega$ SST and $k-\varepsilon$ models with experimental results for $x/D_h = 1.0$; $z/D_h = 0.0$.

Figure 6 represents the components of U/Vc air velocity (Re = 40000) in the cross section of the duct 10 hydraulic diameters $(x/D_h = 10.0;\ z/D_h = 0.0)$

downstream from the duct bend. Experimental results [3] (black filled circles) coincide very well with results obtained in the $k-\omega$ SST turbulence model. It is worth noticing in Fig. 6 that the mentioned profiles of U/Vc velocity components are characterized by a fairly large degree of deformation caused by the bend.

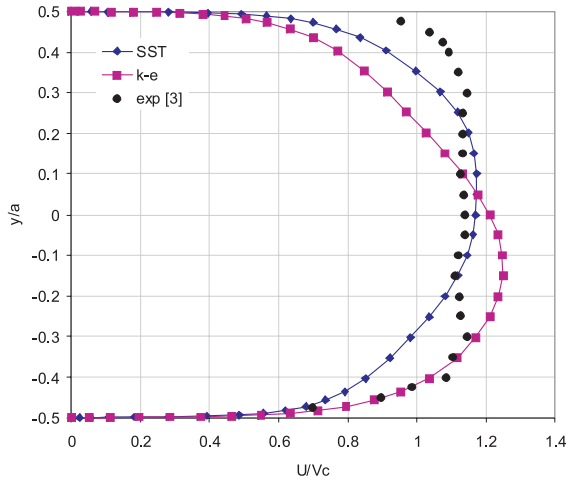

Figure 6. Comparison of velocity profiles obtained with $k-\omega$ SST and $k-\varepsilon$ models with experimental results for $x/D_h = 10.0$; $z/D_h = 0.0$.

Figure 7 shows contours of turbulence intensity (Tu) in the cross section of the duct at five D_h downstream from the bend. In the bottom part of the figure numerical results are presented, whereas in the upper part of the figure corresponding experimental results found in Ref. [3] are shown. In both cases the Reynolds number was Re = 40000. It is worth noticing that the values assigned to the curves describing the changes of Tu correspond closely in both parts of the figure.

Because of good agreement of the obtained numerical results with the corresponding experimental results shown in Figs. 2 to 7 additional simulations were conducted for two flows of air characterized by following values of the Reynolds number; $\mathrm{Re}_2^{(I)} = 54054$ ($U = 10$ m/s) and $\mathrm{Re}_3^{(I)} = 81081$ ($U = 15$ m/s). Obtained numerical results are shown in Figs. 8a, 8b and 8c. Figure 8a presents the profiles of longitudinal component U of velocity in the cross section at angular coordinate $\phi = 30^{\mathrm{o}}$ ($z/D_h = 0.0$). Figures 8b and 8c show similar profiles of U component of velocity obtained for coordinates $\phi = 90^{\mathrm{o}}$ ($z/D_h = 0.,0$) and one hydraulic diameter downstream the bend ($x/D_h = 1.0$; $z/D_h = 0.0$) respectively.

From Figs. 8a, b, and c it can be seen that the maximum value of the U component of air velocity changes its location along the flow. At first for $\phi = 30^{\mathrm{o}}$

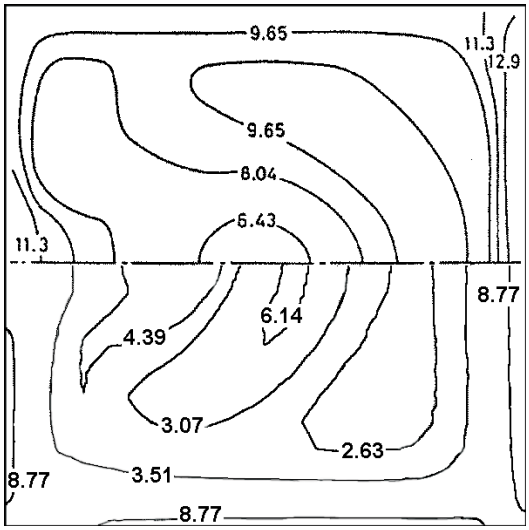

Figure 7. Comparison of contours of turbulence intensity (Tu) at five D_h downstream the duct bend obtained with $k-\omega$ SST model.

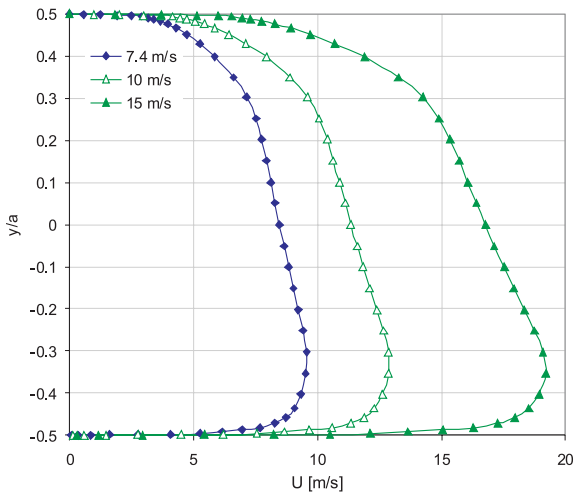

Figure 8. a Comparison of U velocity profiles obtained with $k-\omega$ SST model for 7.4; 10 and 15 m/s for $\phi = 30^{\circ}$ ($z/D_h = 0.0$).

the maximum value of U velocity is located near the inner wall of the bend, then for $\phi = 90^{\circ}$ its maximum is located more towards the center of the duct, whereas in the cross section after the bend is clearly located near the outer wall of the duct. Deformation of the U velocity profile in the discussed flows ($\mathrm{Re}_1^{(I)} = 40000$,

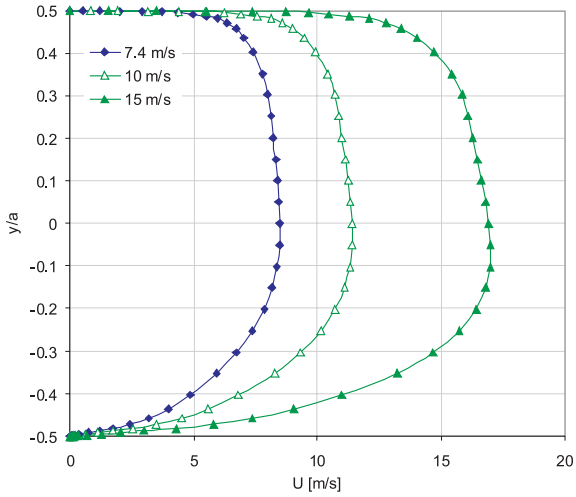

Figure 8. b Comparison of U velocity profiles obtained with $k-\omega$ SST model for 7.4; 10 and 15 m/s for $\phi = 90^{o}$ $(z/D_h = 0, 0)$.

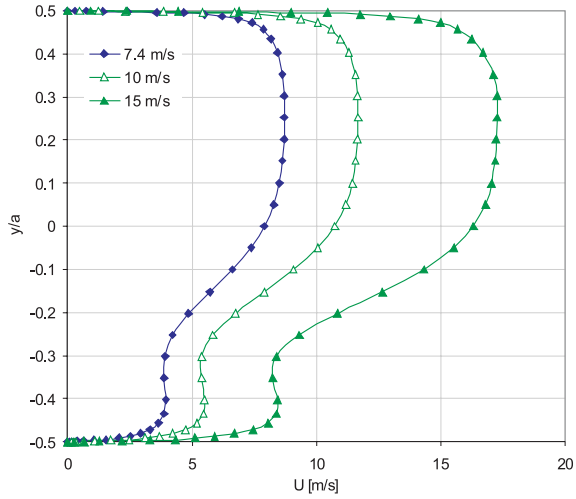

Figure 8. c. Comparison of U velocity profiles obtained with $k-\omega$ SST model for 7.4; 10 and 15 m/s for $x/D_h = 1.0$; $z/D_h = 0.0$.

$\mathrm{Re}_2^{(I)} = 54054$, $\mathrm{Re}_3^{(I)} = 81081$) is clearly visible in cross section located at ten $D_h(x/D_h = 10.0;\ z/D_h = 0.0)$ downstream from the bend.

Figure 9 shows longitudinal velocity components (U/Vc) of water in the cross section located at $2.5D_h(x/D_h = 2.5;\ z/D_h = 0.0)$ downstream the bend of duct

II. Results are presented using the same symbols as in previous figures. In order to compare the obtained results, reference is made to experimental results found in study [2].

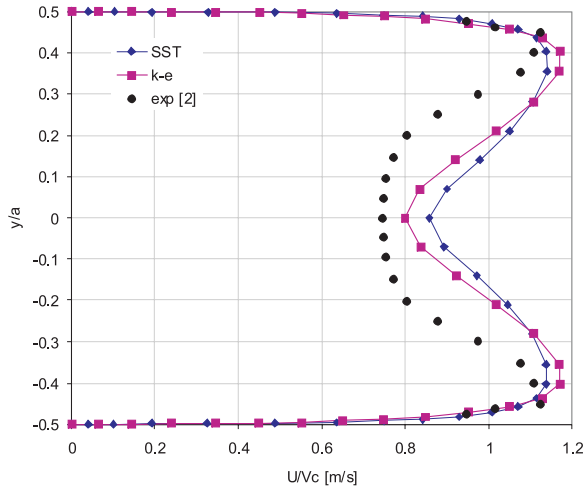

Figure 9. Comparison of longitudinal velocity profiles obtained with $k-\omega$ SST and $k-\varepsilon$ models with experimental results for $x/D_h = 2.5$; $z/D_h = 0.0$.

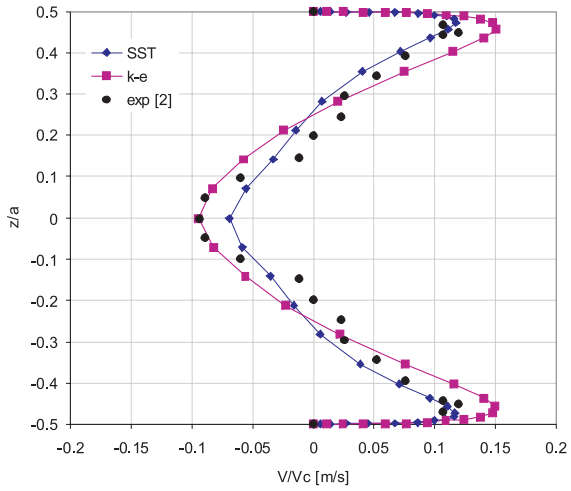

Figure 10. Comparison of cross velocity profiles obtained with $k-\omega$ SST and $k-\varepsilon$ models with experimental results for $x/D_h = 2.5$; $y/D_h = 0.0$.

Corresponding profiles of the cross component of water velocity (V/V_c) in the same cross section of duct II are presented in Fig. 10.

Analysis of numerically obtained curves shown in Figs. 9 and 10 confirms good consistency with experimental results found in Ref. [2]. Figures 11 and 12 present additionally obtained results for numerical calculations in case of greater values of Reynolds and Dean numbers for longitudinal U and cross V velocity components respectively.

Curves denoted with rhombs present results obtained through numerical calculations for $\mathrm{Re}_1^{(II)} = 40000$ ($k-\omega$ SST model). Remaining curves present results of numerical calculations for flows of water characterized by Reynolds numbers; $\mathrm{Re}_2^{(II)} = 60000$ (non filled triangle) and $\mathrm{Re}_3^{(II)} = 80000$ (filled triangle). It is worth noticing that in Fig. 12 presented cross components of V velocity intersect each other at one point located at $z/D_h \approx 0.3$.

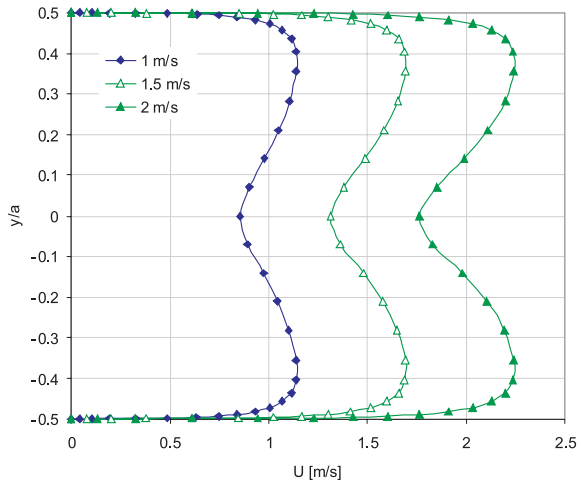

Figure 11. Comparison of longitudinal velocity U profiles obtained numerically with $k-\omega$ SST model for $x/D_h = 2.5$; $z/D_h = 0.0$ for 1.0; 1.5, and 2 m/s.

Figure 13 shows changes of the pressure coefficient C_p on the walls of the bend. The upper curve corresponds to pressure changes on the outer wall: $R_{out} = 112$ mm, whereas the bottom curve corresponds to the inner wall: $R_{in} = 72$ mm. Both curves present results of numerical calculations for $\mathrm{Re} = 40000$ referenced to the center line of the bend wall ($z/D_h = 0.0$). The pressure coefficient is defined exactly as in Ref. [2]:

$$C_p = (\bar{p} - p_{ref})/(\rho V_c^2/2)\,. \tag{8}$$

In order to compare the obtained results shown in Fig. 13 experimental results from Ref. [2] are also included. Only values for the outer wall were available in Ref. [2]. From Fig. 13 it can be seen, that the maximum pressure difference

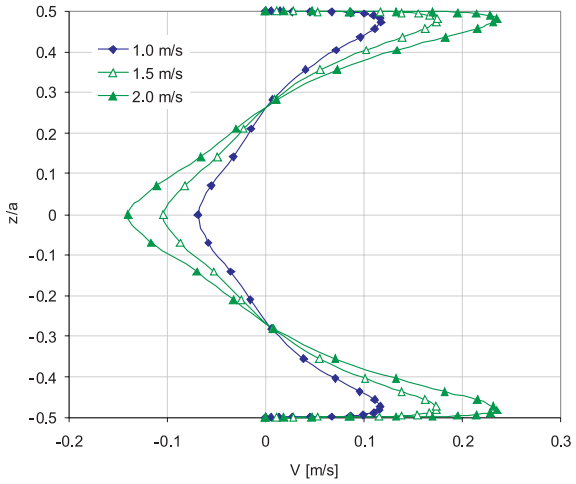

Figure 12. Comparison of cross velocity V profiles obtained numerically with $k-\omega$ SST model for $x/D_h = 2.5$, $y/D_h = 0.0$ for 1.0; 1.5, and 2 m/s.

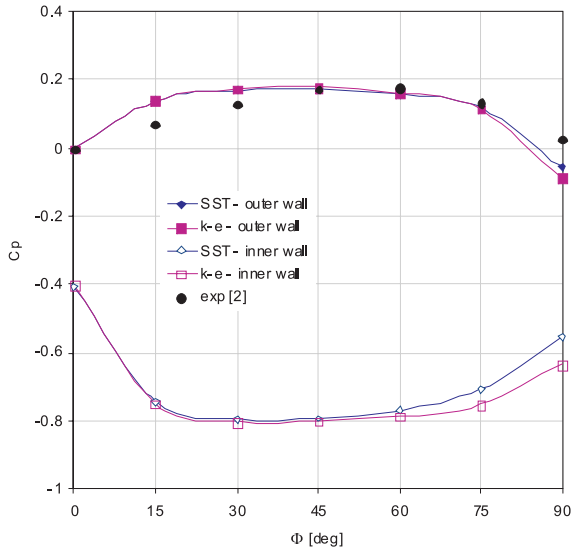

Figure 13. Comparison of pressure coefficient along the bend wall with numerical results obtained with $k-\omega$ SST and $k-\varepsilon$ models.

on the walls of the bend occurs in the cross section described by the angular coordinate $\phi = 45^{\circ}$ ($z/D_h = 0.0$). The mentioned pressure difference is used as a

fundamental parameter for identification of volumetric flow rate through a duct with installed bend with specified dimensions.

4 Conclusions

In the study of numerical simulation of 3D, statistically stationary turbulent flow in a square-sectioned duct with installed bend was carried out. In the calculations the process of formation of velocity profile in the straight inlet section L_{inlet}, preceding the bend, was taken into consideration. The simulation was carried out in FLUENT using two different turbulence models, namely the standard $k-\varepsilon$ and the $k-\omega$ SST turbulence models. Both models allowed achieving results that closely correspond to the experimental results, however results obtained with the $k-\omega$ SST show slightly better qualitative correspondence.

From the analysis of obtained results it seems that in the area upstream of the bend and the first part of the bend ($0^\circ < \phi < 30^\circ$) fluid elements are subjected to significant acceleration in the vicinity of the inner wall of the bend. Simultaneously in the sub-area of the flow close to the outer wall of the bend local rotations of elements are observed, that are responsible for deceleration of the flow. After leaving the bend, the fluid elements experience acceleration in the vicinity of the outer wall. The longitudinal component of the velocity profile is highly deformed after the bend even at distance of $L_{outlet} \approx 10D_h$ down stream the bend of the analyzed flow. From obtained numerical results it seems that the discussed section of the deformed flow is slightly shorter in case of flow of water that is for higher fluid viscosity.

The discussed section of the duct downstream of the bend (L_{outlet}) has significant meaning in case of installation of measuring instruments, for example, measuring orifice, Prandtl tube and other contributing to high errors of measurements. Based on the analysis of the obtained results it can be stated that the velocity field is more sensitive to disturbances caused by the installed bend than the corresponding pressure field. It seems that the measured pressure difference at the extremes of the secant of the bend of a rectangular duct might be a parameter used for identification of the volumetric flow rate similarly as for bends installed in pipes (circular ducts) [9].

Acknowledgement The research financed from scientific grants in the years 2007-2010 conducted as a research project.

Received 10 December 2007

References

[1] Ito H.: *Flow in curved pipes*, JSME International Journal, Vol. 30, No. 262, 1987, 161-171.

[2] Taylor A.M.K.P., WhitelawJ .H., Yianneskis M.: *Curved ducts with strong secondary motion: Velocity measurements of developing laminar and turbulent flow*, Transactions of ASME J. Fluids Eng., Vol. 104, 1982, 350-359.

[3] Sudo K., Sumida M., Hibara H.: *Experimental investigation on turbulent flow in a square-sectioned 90-degree bend*, Experiments in Fluids, 30, 2001, 246-252.

[4] Song B., Amado R.S.: *Application of non-linear k-ω model to a turbulent flow inside a sharp U-bend*, Computational Mechanics, 26, 2000, 344-351.

[5] Ng Y. T., Luo S.C., Lim T.T.,Ho Q.W.: *On swirl development in a square cross-sectioned, S-shaped duct*, Exp Fluids, 41, 2006, 975-989.

[6] Fluent 6.1 Users Guide, Fluent Inc. 2004.

[7] Wilcox D.C.: *Turbulence Modeling for CFD*, DCW. Industries, Anaheim, Third Ed. 2006.

[8] Pope S.B.: *Turbulent Flows*, Cambridge Univ. Press, Cambridge 2000.

[9] Rup K., Malinowski L.: *Fluid flow identification on base of the pressure difference measured on the secant of a pipe elbow.* Forschung im Ingenieurwesen (2006) 70: 199-206.